Potential-Dependent Adsorption and Orientation of meso-Substituted Porphyrins at Liquid|Liquid Interfaces Studied by Polarization-Modulation Total Internal Reflection Fluorescence Spectroscopy

Potential-Dependent Adsorption and Orientation of *meso*-Substituted Porphyrins at Liquid|Liquid Interfaces Studied by Polarization-Modulation Total Internal Reflection Fluorescence Spectroscopy

Sho Yamamoto,[†] Hirohisa Nagatani,*[,‡] Kotaro Morita[‡] and Hisanori Imura[‡]

[†] Division of Material Chemistry, Graduate School of Natural Science and Technology, Kanazawa University, Kakuma, Kanazawa 920-1192, Japan

[‡] Faculty of Chemistry, Institute of Science and Engineering, Kanazawa University, Kakuma, Kanazawa 920-1192, Japan

*To whom correspondence should be addressed: H. Nagatani

Tel: +81 76 264 5692; FAX: +81 76 264 6059; E-mail: nagatani@se.kanazawa-u.ac.jp

ABSTRACT

Potential-dependent adsorption behavior of *meso*-substituted water-soluble porphyrins at the polarized water|1,2-dichloroethane (DCE) interface was studied by polarization-modulation total internal reflection fluorescence (PM-TIRF) spectroscopy. In the PM-TIRF experiments, the fluorescence signal from the interfacial region was analyzed as a function of the periodic modulation of linear-polarizations (s and p) of the incident excitation beam. The potential-dependence of PM-TIRF responses for *meso*-substituted porphyrins, 5,10,15,20-tetrakis(*N*-methylpyridyl)porphyrin (H_2TMPyP^{4+}) and 5,10,15,20-tetrakis(4-sulfonatophenyl)porphyrin (H_2TPPS^{4-}) indicated that both free base porphyrins were adsorbed with relatively lying orientations at the polarized water|DCE interface. The average orientation angles (θ) were estimated as $\theta = 61 \pm 1°$ for H_2TMPyP^{4+} and $\theta = 65 \pm 1°$ for H_2TPPS^{4-} with respect to the interface normal. The wavelength-dependence of polarization-modulated fluorescence signals (PM-TIRF spectrum), which corresponds to "pure" emission spectrum of interfacial species, clearly indicated that H_2TMPyP^{4+} and H_2TPPS^{4-} are adsorbed with a modification of the solvation at the interface. These results demonstrated a high ability of the PM-TIRF spectroscopy for the direct characterization of fluorescent species adsorbed at polarized liquid|liquid interfaces.

INTRODUCTION

An interface between two immiscible electrolyte solutions (ITIES) is a two-dimensional specific reaction field, where charge transfer processes are controlled as a function of the Galvani potential difference between two phases ($\Delta_o^w\phi$).[1-2] The heterogeneous reaction at ITIES often involves the interfacial adsorption process of reactants. The interfacial mechanism and kinetics are then significantly affected by the adsorption state of the reactants. The detailed characterizations of interfacial species at molecular level such as solvation structure, molecular orientation and intermolecular interaction are important to elucidate the heterogeneous reaction mechanism.[3-4] However, it is extremely difficult to characterize the interfacial species *in situ* by using conventional spectroscopies since ion transfer reactions (or ion partitioning) could take place simultaneously with their adsorption processes at ITIES. In such cases, weak signals of the interfacial species cannot readily be differentiated from bulk solution species. Total internal reflection (TIR) spectroscopy is one of the most powerful techniques to investigate the reaction mechanism at ITIES.[5-6] In particular, total internal reflection fluorescence (TIRF) spectroscopy has provided various insights of interfacial species with its high sensitivity.[7-9] In TIRF spectroscopy, the fluorescent dye species located in evanescent wave region are excited by the incident beam from a high refractive index medium. When dye species are dissolved in the incident medium, however, the optical signals from the interfacial region are relatively weaken and buried in strong signals from the bulk solution species. Surface second harmonic generation (SSHG) spectroscopy is extremely sensitive to molecules adsorbed at the interface between two centrosymmetric phases such as liquid surfaces, solid|liquid and liquid|liquid interfaces.[10-16] In the electric dipole approximation, the second harmonic (SH) signal is only generated from oriented molecules adsorbed at the interface. Although SSHG spectroscopy is a quite useful technique to characterize interfacial species with high selectivity, the self-absorption of SH signals by bulk species at resonant wavelengths through the optical path remains a serious problem. The requirements of a high power laser system and a strict optical setup may also reduce general versatility of this technique.

Modulation techniques have been combined with the TIR spectroscopy in order to enhance selectivity for interfacial species.[17-18] At polarized liquid|liquid interfaces, the transfer and adsorption processes of ionic species are controlled as a function of $\Delta_o^w\phi$ and thus an ac potential-modulation applied to the interface induces a perturbation of spectroelectrochemical signal arising from the interfacial region. Potential-modulation spectroscopy has been employed to analyze the charge transfer reaction at liquid|liquid interfaces,[5, 19-20] in which the high sensitivity of potential-modulated fluorescence (PMF) spectroscopy has enabled us to study the interfacial mechanism of various fluorescent species.[21-26] In PMF measurements, the ion transfer and adsorption processes are distinguishable through the complex analysis of PMF signals within the framework of simple phenomenological models at a polarized liquid|liquid interface.[27] The direct characterization of interfacial species was also achieved under limited conditions. The sensitivity and selectivity for the adsorbed species are still insufficient in the case that the transfer and adsorption processes takes place in the same potential region.

Polarization modulation infrared reflection absorption spectroscopy (PM-IRRAS) has been used to determine the molecular orientation and the conformation of layered materials formed at solid and liquid surfaces.[28-32] In PM-IRRAS, the linear polarizations of the incident light are periodically modulated and selectivity for oriented species is drastically improved by analyzing corresponding ac optical signals. A similar approach has also been applied to total reflection X-ray absorption fine structure (TR-XAFS) at liquid surfaces and liquid|liquid interfaces.[33-35] Polarized TR-XAFS measurements, where the linear polarization of incident X-rays is controlled by a diamond retarder crystal, allowed us to estimate the solvation structure of metalloporphyrins at interfaces *in situ*.[36-38] However, the application of PM-IRRAS and polarized TR-XAFS to liquid|liquid systems is rigidly limited by strong attenuation or scattering of incident beam and optical signal by solvent molecules in infrared and X-ray regions.

In the present study, we developed polarization-modulation total internal reflection fluorescence (PM-TIRF) spectroscopy to study adsorbed species at liquid|liquid interfaces. PM-TIRF spectroscopy can effectively extract the fluorescence responses of the molecules oriented

at the interface buried in the signals arising throughout the optical path in the incident medium. PM-TIRF spectroscopy was applied to *meso*-substituted water-soluble porphyrins, 5,10,15,20-tetrakis(*N*-methylpyridyl)porphyrin (H_2TMPyP^{4+}) and 5,10,15,20-tetrakis(4-sulfonatophenyl)porphyrin (H_2TPPS^{4-}) at the polarized water|1,2-dichloroethane (DCE) interface. The dependences of PM-TIRF signals on $\Delta_o^w\phi$ and PM-TIRF spectra at given potentials clarified the interfacial behavior of those free base porphyrins in detail.

EXPERIMENTAL SECTION

Reagents. 5,10,15,20-tetrakis(*N*-methylpyridyl)porphyrin (H_2TMPyP^{4+}) tetratosylate salt and 5,10,15,20-tetrakis(4-sulfonatophenyl)porphyrin (H_2TPPS^{4-}) disulfuric acid tetrahydrate were purchased from Dojindo Laboratories and used as received. The composition of the electrochemical cell is represented in **Figure 1**. The concentrations of H_2TMPyP^{4+} and H_2TPPS^{4-} in the aqueous phase were 2.0×10^{-5} mol dm^{-3}. The supporting electrolytes were 1.0×10^{-2} mol dm^{-3} LiCl for the aqueous phase and 5.0×10^{-3} mol dm^{-3} bis(triphenylphosphoranylidene)ammonium tetrakis(pentafluorophenyl)borate (BTPPATPFB) for the organic phase, respectively. BTPPATPFB was prepared by metathesis of bis(triphenylphosphoranylidene)ammonium chloride (BTPPACl) (Aldrich, >97%) and lithium tetrakis(pentafluorophenyl)borate ethyl ether complex (TCI, ≥70%). The aqueous solutions were prepared with purified water by a Milli-Q system (Millipore, Direct-Q3UV). 1,2-dichloroethane (DCE) (Nacalai Tesque, HPLC grade, >99.7%) was used as an organic solvent. DCE and water were saturated with each other. All other reagents used were of analytical grade or higher. The pH of the aqueous phase was controlled by 1.0×10^{-3} mol dm^{-3} LiH_2PO_4/LiOH buffer for neutral conditions.

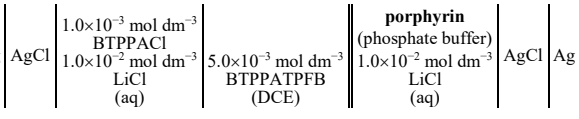

Figure 1. Composition of the electrochemical cell.

Spectroelectrochemical Setup. The spectroelectrochemical cell used in all measurements was analogous to one reported previously (**Figure 2**).[17] The water|DCE interface with a geometrical area of 0.50 cm^2 was polarized by a four-electrode potentiostat (Hokuto Denko, HA-1010mM1A). The platinum counter (CE) and reference electrodes (RE: Ag/AgCl with Luggin capillary) were used in both phases. The Galvani potential difference ($\Delta_o^w\phi \equiv \phi^w - \phi^o$) was estimated by taking the formal transfer potential ($\Delta_o^w\phi^{o\prime}$) of tetramethylammonium ions as −0.160 V.[39] The water|DCE interface was illuminated under the total internal reflection (TIR) condition from organic phase by a cw laser diode at 404 nm (Coherent, CUBE 405-50C, 50 mW). The critical angle for the water|DCE interface is 67.6° and the angle of incidence to the interface (α) was ca. 75°. The laser radiation was attenuated to 25 mW to avoid the photobleaching of porphyrins. The fluorescence emitted from the interfacial region was collected perpendicularly to the interface by an optical fiber fitted to a photomultiplier tube (PMT) through a monochromator (Shimadzu, SPG-120S). The linear polarization of incident excitation beam was periodically modulated from p- (parallel to the plane of incidence) to s-polarization (perpendicular to the plane of incidence) at 13 Hz by a liquid crystal retarder (LCR) thermostated at 323 K (Thorlabs, LCC1111T-A, LCC25/TC200). The polarization modulation efficiency (P_m) of LCR was defined as the fraction of the p- or s-polarized component in the excitation beam under respective light

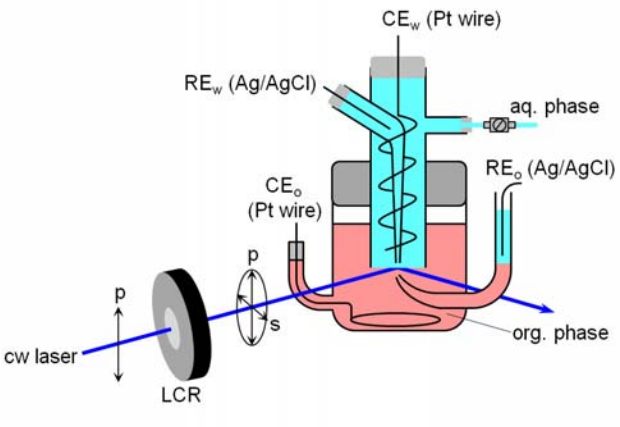

Figure 2. Schematic drawing of the spectroelectrochemical setup for PM-TIRF measurement.

modulations and measured as P_m = 0.95 by a Glan Thompson prism (Sigma Koki, GTPC-10-33SN) and a Si photodiode (Hamamatsu Photonics, S1133-01) (cf. Supporting Information: **S1**). The polarization-modulated fluorescence signal was analyzed by a digital lock-in amplifier (NF, LI5640) as a function of periodic modulation of linear polarizations. $\Delta_o^w\phi$ was linearly swept at 5 mV s^{-1} for potential dependence measurements. All experiments were carried out in a thermostated room at 298 ± 2 K.

Polarization-Modulation Total Internal Reflection Fluorescence (PM-TIRF) Response. The fluorescence intensity emitted form a molecule adsorbed at an interface is determined by the molecular orientation and polarizations of the excitation beam. Assuming that a transition dipole moment is considered in a molecular axis, the fluorescence intensity from a molecule oriented at an angle (θ) with respect to the interface normal can be given by[21, 40-41]

$$F(\Psi) = C[\sin^2\theta\cos^2(90° - \Psi) + (\cos^2\alpha\sin^2\theta + 2\sin^2\alpha\cos^2\theta)\sin^2(90° - \Psi)] \quad (1)$$

where Ψ is the angle of polarization of excitation beam with respect to the normal to the interface and C is a proportional factor. The Ψ values for the p- and s-polarized excitation beams are 0° and 90°, respectively. **Figure 3** schematically illustrates the polarization angle

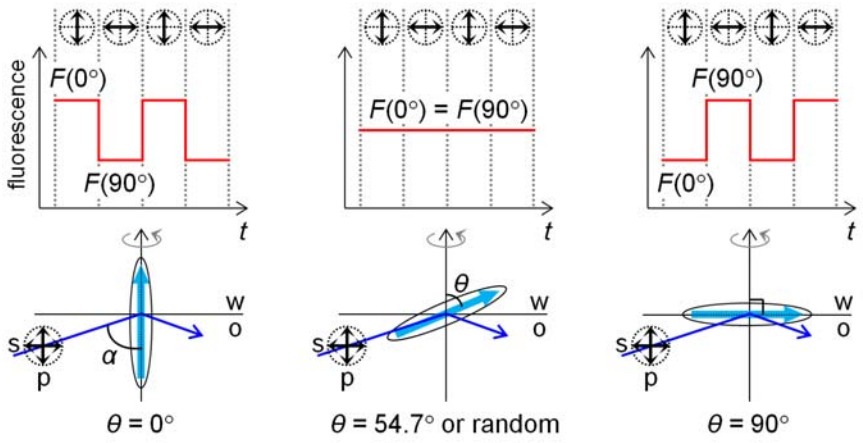

Figure 3. Schematic representation of the fluorescence signal from molecules oriented at θ. The polarization angle (Ψ) of incident excitation beam is periodically modulated between 0° (p) and 90° (s).

dependence of the fluorescence intensity $F(\Psi)$ under TIR conditions. The intensity of $F(0°)$ under the p-polarized excitation for molecules oriented at $0° \le \theta < 54.7°$ is larger than $F(90°)$ under the s-polarized excitation, while an opposite relationship is obtained in the case of $54.7° < \theta \le 90°$. At $\theta = 54.7°$ or random orientation, the fluorescence intensity is constant irrespective of Ψ, i.e. $F(0°) = F(90°)$ (cf. Supporting Information: **Figure S2**). In the present work, the PM-TIRF signal ($\Delta F^{\text{p-s}}$) is defined as

$$\Delta F^{\text{p-s}} = F(0°) - F(90°) \tag{2}$$

When the modulation efficiency (P_{m}) is not equal to 1, the excitation beam consists of both the p- and s-polarized components under polarization modulation. The total intensities of the modulated fluorescence in the p- and s-polarization modes, F_{m}^{p} and F_{m}^{s}, can be represented by

$$F_{\text{m}}^{\text{p}} = P_{\text{m}} F(0°) + (1 - P_{\text{m}}) F(90°) \tag{3}$$

$$F_{\text{m}}^{\text{s}} = P_{\text{m}} F(90°) + (1 - P_{\text{m}}) F(0°) \tag{4}$$

From eqs. 3 and 4, $\Delta F^{\text{p-s}}$ with $P_{\text{m}} < 1$ is rewritten as

$$\Delta F^{\text{p-s}} = F_{\text{m}}^{\text{p}} - F_{\text{m}}^{\text{s}} = (2P_{\text{m}} - 1)\big(F(0°) - F(90°)\big) \tag{5}$$

The signs of $\Delta F^{\text{p-s}}$ can be diagnostic criteria for the relative orientation of interfacial molecule, in which positive and negative values indicate relatively standing and lying molecular orientations with respect to interface (cf. Supporting Information: **Figure S3**). When the molecules are adsorbed at the interface with $\theta = 54.7°$ or random orientation, $\Delta F^{\text{p-s}}$ should be zero. In PM-TIRF spectroscopy, the fluorescence signal arising from bulk solution species with random orientation is effectively cancelled out by periodic polarization modulation, and PM-TIRF spectroscopy is thus highly sensitive and selective to the interfacial species with a certain orientation.

RESULTS AND DISCUSSION

Interfacial Adsorption and Orientation Behavior of Porphyrins. Figure 4 shows cyclic voltammograms (CVs) measured in the presence of 2.0×10^{-5} mol dm^{-3} H_2TMPyP^{4+} and H_2TPPS^{4-} under neutral conditions, where both porphyrins exist as the free base form in the aqueous solution. The well-defined voltammetric responses were observed in each system. In **Figure 4a**, the positive and negative current peaks obtained for H_2TMPyP^{4+} correspond to the diffusion controlled ion transfer of tetracationic species from water to DCE and that of the reverse process across the interface, respectively, since the peak currents exhibited a linear relationship with square root of potential sweep rate. The formal ion transfer potential of H_2TMPyP^{4+} was determined as $\Delta_o^w\phi^{\circ'}_{H_2TMPyP^{4+}} = 0.07$ V. The current increases at the negative edge of potential window is attributed to the ion transfer of tosylate anions ($\Delta_o^w\phi^{\circ'}_{tosylate} = -0.28$ V) as a counter ion of H_2TMPyP^{4+}.[42] The ion transfer responses of H_2TPPS^{4-} were obtained at $\Delta_o^w\phi^{\circ'}_{H_2TPPS^{4-}} = -0.20$ V (**Figure 4b**). In addition, the broad positive current responses at $0.25\text{ V} < \Delta_o^w\phi < 0.30\text{ V}$ and the gradual increase of currents prior to the ion transfer ($\Delta_o^w\phi < 0.10$ V) were observed for H_2TMPyP^{4+} and H_2TPPS^{4-}, respectively (see also Supporting Information: **Figure S4**). These additional voltammetric responses are in accord with our previous reports, in which the PMF analysis elucidated the transfer mechanism of the free base porphyrins accompanied by the specific adsorption at either side of the water|DCE interface.[22]

The PM-TIRF spectroscopy was employed to study the potential dependent adsorption behavior of the porphyrins in detail at the water|DCE interface. **Figures 5a** and **6a** show the potential dependences of PM-TIRF signals, $\Delta F^{p\text{-}s}$, measured in the H_2TMPyP^{4+} and H_2TPPS^{4-}systems, respectively. The PM-TIRF responses were recorded at 660 nm for H_2TMPyP^{4+} and 649 nm for H_2TPPS^{4-}, respectively, where these porphyrins emit relatively strong fluorescence in both aqueous and organic solutions under present excitation conditions. In principle, the PM-TIRF signal is observed only from the species adsorbed at the interface with a

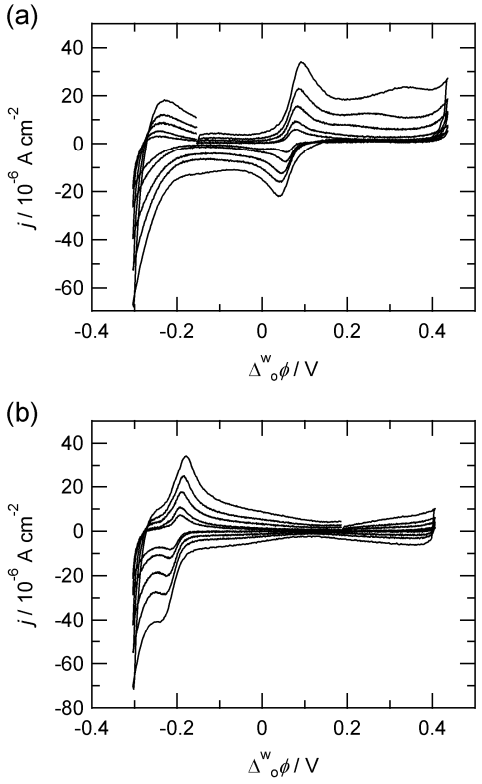

Figure 4. Typical cyclic voltammograms measured for (a) H_2TMPyP^{4+} and (b) H_2TPPS^{4-} at the water|DCE interface. The potential sweep rates were 10, 20, 50, 100 and 200 mV s^{-1}. The concentration of porphyrin derivatives in the aqueous phase was 2.0×10^{-5} mol dm^{-3}. The pH values of the aqueous phase were (a) pH 7.1 and (b) pH 6.9, respectively.

certain orientation (cf. **Figure 3** and experimental data for tris(2,2′-bipyridine)ruthenium(II) ($Ru(bpy)_3^{2+}$) in Supporting Information: **S4**). The nonzero $\Delta F^{\text{p-s}}$ values are, therefore, indicative of a selective detection of the species oriented at the interface. The potential dependence of $\Delta F^{\text{p-s}}$ is useful in evaluating the molecular orientation of the interfacial species as a function of $\Delta_o^w\phi$. As shown in **Figure 5a** and **6a**, the negative PM-TIRF signals, $-\Delta F^{\text{p-s}} > 0$, were observed over the potential window, suggesting that both porphyrin species were adsorbed with relatively lying orientations at the polarized water|DCE interface. For the π–π* transition in porphyrin systems, the two absorption and respective emission transition dipole moments are perpendicular to each

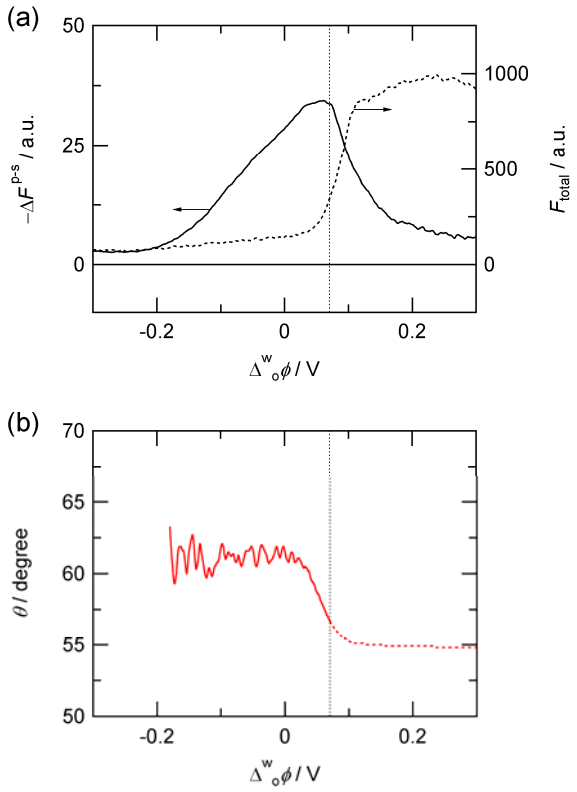

Figure 5. The potential dependence of (a) PM-TIRF responses ($\Delta F^{p\text{-}s}$) (solid) and F_{total} (dashed) and (b) the orientation angles (θ) estimated from eqs. 6, 8 and 9 for H_2TMPyP^{4+} system. The potential sweep rate was 5 mV s^{-1}. The fluorescence intensity was detected at 660 nm. The vertical dotted lines depict $\Delta^{w}_{o}\phi^{o'}_{H_2TMPyP^{4+}} = 0.07$ V.

other and parallel to the porphyrin ring (in plane).[43] Hence, the orientation of a molecule is considered as equal to that of a porphyrin ring. The average orientation angle (θ) of interfacial species can be expressed by eq. 1, assuming a monodispersed distribution of θ. To cancel the proportional value C in eq. 1, the θ value is determined by the ratio of $F(90°)$ to $F(0°)$

$$\frac{F(90^\circ)}{F(0^\circ)} = \frac{\sin^2\theta}{\cos^2\alpha\sin^2\theta + 2\sin^2\alpha\cos^2\theta} \qquad (6)$$

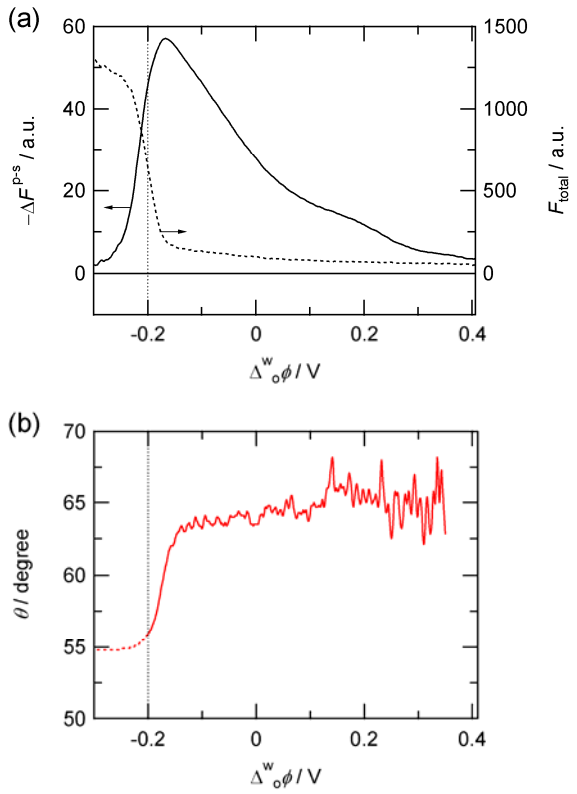

Figure 6. The potential dependence of (a) PM-TIRF responses ($\Delta F^{\text{p-s}}$) (solid) and F_{total} (dashed) and (b) the orientation angles (θ) estimated from eqs. 6, 8 and 9 for H_2TPPS^{4-} system. The potential sweep rate was 5 mV s^{-1}. The fluorescence intensity was detected at 649 nm. The vertical dotted lines depict $\Delta^{\text{w}}_{\text{o}}\phi^{\circ'}_{\text{H}_2\text{TPPS}^{4-}} = -0.20\,\text{V}$.

The individual magnitudes of $F(90°)$ and $F(0°)$ were estimated from eq. 5 and total fluorescence intensity (F_{total}). F_{total} includes the fluorescence emitted from all species existing in the interfacial region and bulk solution phases.

$$F_{\text{total}} = \frac{1}{2}\left(F_{\text{m}}^{\text{p}} + F_{\text{m}}^{\text{s}}\right) + F_{\text{bulk}} = \frac{P_{\text{m}}}{2}\left(F(0°) + F(90°)\right) + F_{\text{bulk}} \qquad (7)$$

where the F_{bulk} term arises from only the randomly oriented bulk solution species in the evanescent wave region at the aqueous side of the interface and on the optical path of the excitation beam in the bulk organic phase. The F_{total} value was measured as the mean value of fluorescence intensities obtained by p- and s-polarized excitation beams at a given potential

(**Figure 5a** and **6a**). Then, $F(0°)$ and $F(90°)$ for the molecules adsorbed at the interface are expressed by the following equations derived from eqs. 5 and 7.

$$F(0°) = \frac{1}{P_m}(F_{total} - F_{bulk}) + \frac{1}{4P_m - 2}\Delta F^{p\text{-}s} \quad (8)$$

$$F(90°) = \frac{1}{P_m}(F_{total} - F_{bulk}) - \frac{1}{4P_m - 2}\Delta F^{p\text{-}s} \quad (9)$$

The fluorescence intensity associated with bulk organic species was negligible except at potentials beyond $\Delta_o^w\phi^{\circ\prime}$ (Supporting Information: **S4**). Accordingly, the significant increases of F_{total} around $\Delta_o^w\phi^{\circ\prime}$ is due to the bulk solution species transferred into the organic phase. The F_{bulk} values from the evanescent wave region in the aqueous phase were roughly estimated from F_{total} at −0.30 V ($< \Delta_o^w\phi^{\circ\prime}_{H_2TMPyP^{4+}} = 0.07$ V) for H_2TMPyP^{4+} and 0.41 V ($> \Delta_o^w\phi^{\circ\prime}_{H_2TPPS^{4-}} = -0.20$ V) for H_2TPPS^{4-}, where their interfacial adsorption and ion transfer are negligibly small. The $F(0°)$ and $F(90°)$ values in the absence of the fluorescent species in the organic phase, therefore, can be calculated by eqs. 8 and 9 with F_{total}, $\Delta F^{p\text{-}s}$ and estimated F_{bulk} values.

The average orientation angles of H_2TMPyP^{4+} estimated from eqs. 6, 8 and 9 is shown in **Figure 5b**. The θ values at $-0.18\text{ V} \le \Delta_o^w\phi \le 0\text{ V}$ were almost constant at $61 \pm 1°$. The magnitude of $\Delta F^{p\text{-}s}$ is proportional to the interfacial concentration, when the θ value is constant. Thus, a gradual increase of $-\Delta F^{p\text{-}s}$ at $\Delta_o^w\phi < \Delta_o^w\phi^{\circ\prime}_{H_2TMPYP^{4+}}$ associates with the increase of the interfacial concentration of H_2TMPyP^{4+} depending on the potential. On the other hand, the drastic decrease of $-\Delta F^{p\text{-}s}$ at $\Delta_o^w\phi^{\circ\prime}_{H_2TMPYP^{4+}} < \Delta_o^w\phi$ results from the ion transfer of H_2TMPyP^{4+} into the organic phase. The interfacial concentration of ionic species is significantly affected by $\Delta_o^w\phi$ and maximized around $\Delta_o^w\phi^{\circ\prime}$ as expected from simple adsorption models.[27, 44-45] The potential dependence of PM-TIRF intensity observed in the present work agreed with those theoretical models. Although the negative $\Delta F^{p\text{-}s}$ values at $\Delta_o^w\phi^{\circ\prime}_{H_2TMPYP^{4+}} < \Delta_o^w\phi$ indicate the

adsorption of H_2TMPyP^{4+} with a relatively lying orientation at the interface, the θ value could not be estimated quantitatively because of nonconstant F_{bulk} arising from H_2TMPyP^{4+} partitioned into the bulk organic phase. Indeed, the significant increase of F_{total} (cf. **Figure 5a**), which is mainly correlated to F_{bulk} from the bulk organic species on the optical path, was observed at corresponding potentials. The PM-TIRF responses of H_2TMPyP^{4+} were slightly changed in the presence of nonionic surfactant, sorbitan monolaurate (Span 20) which is commonly used as a stabilizer for the electrochemical measurements in the liquid|liquid system in order to minimize the convection of the solutions in the vicinity of the interface.[22-23] As described in Supporting Information: **Figure S7**, the estimated θ values at $-0.05\,\mathrm{V} \le \Delta_o^w\phi \le 0.05\,\mathrm{V}$ showed relatively large values in the presence of Span 20 in the organic phase, indicating that the addition of nonionic stabilizer certainly affects the adsorption state of ionic analyte molecules at the interface.

The PM-TIRF signals measured in the H_2TPPS^{4-} system (**Figure 6**) were analyzed in the same manner described above. The nonzero $\Delta F^{p\text{-}s}$ was clearly observed even at 0.30 V which was 0.5 V more positive potential than $\Delta_o^w\phi^{o'}_{H_2TPPS^{4-}}$, indicating the high affinity to the water|DCE interface (**Figure 6a**). The θ values for H_2TPPS^{4-} at $-0.10\,\mathrm{V} \le \Delta_o^w\phi \le 0.35\,\mathrm{V}$ were approximately constant at $65 \pm 1°$ (**Figure 6b**). The negative magnitude of $\Delta F^{p\text{-}s}$ values were remarkably decreased at $\Delta_o^w\phi < \Delta_o^w\phi^{o'}_{H_2TPPS^{4-}}$ and almost zero around −0.30 V. These results indicated that H_2TPPS^{4-} is adsorbed mainly from the aqueous side of the interface prior to the formal ion transfer potential.

PM-TIRF Spectra of Porphyrins Adsorbed at Polarized Water|DCE Interfaces. The wavelength-dependence of polarization-modulated fluorescence intensity, i.e. PM-TIRF spectrum, was measured in order to characterize the adsorption state of the porphyrin species at the polarized water|DCE interface. Since PM-TIRF signals result from only the fluorescent dyes with a certain orientation, spectral contributions of randomly oriented species are negligible. The

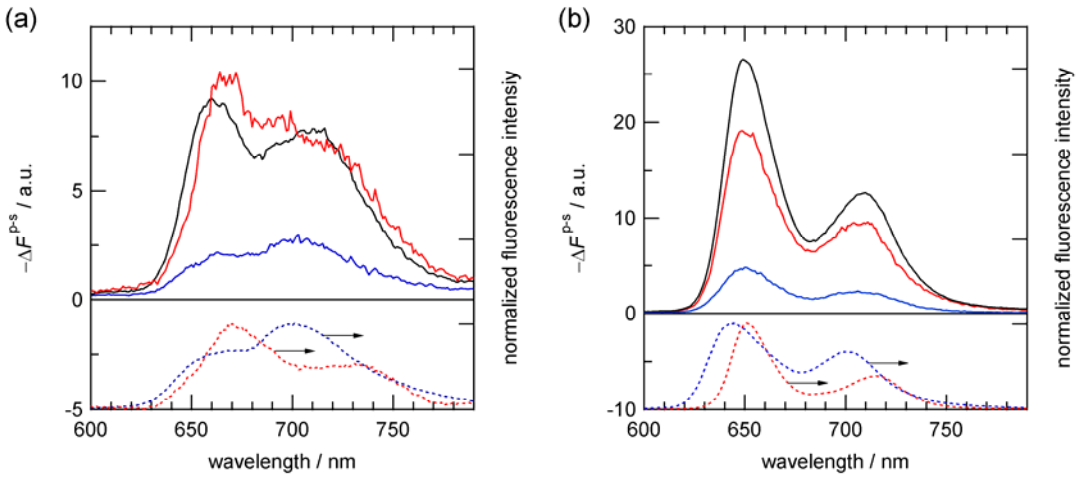

Figure 7. PM-TIRF spectra for (a) H_2TMPyP^{4+} and (b) H_2TPPS^{4-} at the water|DCE interface. (a) The blue, black and red solid lines depict PM-TIRF spectra at −0.27 V, −0.15 V and 0.19 V, respectively. (b) The blue, black and red solid lines depict PM-TIRF spectra at 0.31 V, −0.10 V and −0.21 V, respectively. The blue and red dashed lines refer to normalized fluorescence spectra measured in the aqueous and organic solutions.

PM-TIRF spectrum is, thus, considered a "pure" emission spectrum of interfacial species oriented at the interface. **Figure 7** shows the PM-TIRF spectra for H_2TMPyP^{4+} and H_2TPPS^{4-} at the water|DCE interfaces under potentiostatic control. The fluorescence maximum wavelengths (λ_{max}) and peak intensity ratios of the first and second peaks (R_F) of PM-TIRF spectra are summarized in **Table 1**.

The PM-TIRF spectra in the H_2TMPyP^{4+} system were measured at –0.27 V, –0.15 V and 0.19 V, respectively (**Figure 7a**). The spectral shape and fluorescence maxima of the PM-TIRF spectra at –0.27 V and 0.19 V were similar to those of the fluorescence spectra measured in the aqueous and organic solutions, respectively. Taking into account $\Delta^{w}_{o}\phi^{o'}_{H_2TMPyP^{4+}} = 0.07$ V, H_2TMPyP^{4+} is stably located in the aqueous phase at –0.27 V, while it is transferred into the organic phase across the interface at 0.19 V. Therefore, the PM-TIRF spectra measured at –0.27 V and 0.19 V associate with H_2TMPyP^{4+} adsorbed at the aqueous and organic sides of the

Table 1. Fluorescence maximum wavelengths (λ_{max}) and peak ratios (R_F) of H_2TMPyP^{4+} and H_2TPPS^{4-} at the water|DCE interface and in solution.

	H_2TMPyP^{4+} system			H_2TPPS^{4-} system		
	$\Delta_o^w\phi$ / V	λ_{max} / nm	R_F[a]	$\Delta_o^w\phi$ / V	λ_{max} / nm	R_F[a]
interface	0.19	668, 720	1.4	0.31	650, 707	2.1
	–0.15	660, 710	1.2	−0.10	649, 709	2.1
	–0.27	660, 702	0.76	−0.21	649, 709	2.1
aqueous phase[b]		660, 702	0.69		644, 701	1.5
organic phase[b]		670, 727	1.6		652, 715	2.5

[a]The peak intensity ratio of the first and second fluorescence peaks. [b]The fluorescence maximum wavelengths measured in the aqueous and organic solutions.

interface. The comparable spectral features of PM-TIRF spectra with relevant bulk spectra exhibit similar solvation states of interfacial species and bulk solution species. On the other hand, the PM-TIRF spectrum measured at –0.15 V was slightly modified from the bulk aqueous spectrum in spite of $\Delta_o^w\phi < \Delta_o^w\phi^{o'}_{H_2TMPyP^{4+}}$. The PM-TIRF maxima were found at around 660 nm and 710 nm at –0.15 V and the peak ratio indicated intermediate value between those of the bulk aqueous and organic spectra. It is reported that the spectral shape and fluorescence maxima of H_2TMPyP^{4+} dissolved in various solvents are affected by polarity of solvents.[46] It has been demonstrated that the solvatochromic dye species located in the interfacial region are influenced from the aqueous and organic solvents, where the spectral features often indicate specific solvation at the interface.[12, 47-52] In our previous studies,[22, 42, 53] the spectral shifts of adsorbed species were observed for the free base and zinc(II) porphyrins at polarized water|DCE interfaces through SSHG and PMF techniques. The potential-dependence of the interfacial species has, however, rarely been studied in detail because of relatively long data acquisition time and/or unfavorable contributions from the partition and ion transfer across the interface. The spectral

features at −0.15 V measured in the present study could be associated with an intermediate solvation structure of H_2TMPyP^{4+} adsorbed at the interface. As described previously, the average orientation angle of H_2TMPyP^{4+} was increased at around $\Delta_o^w\phi^{o'}_{H_2TMPyP^{4+}}$ in the presence of Span 20 (cf. Supporting information: **Figure S7**). The interfacial species was also affected by Span 20, in which the PM-TIRF spectra were identical to the bulk organic spectrum even at −0.27 V, suggesting that Span 20 interacts with H_2TMPyP^{4+} molecules at the interface (cf. Supporting Information: **Figure S8** and **Table S1**). The PM-TIRF spectra similar to the bulk organic spectrum over the measurable potential region ($-0.27\,V \le \Delta_o^w\phi \le 0.19\,V$) imply a dehydration of the porphyrin ring induced by sorbitan moiety of Span 20 penetrated into the aqueous side of the interface.

The PM-TIRF spectra measured in the H_2TPPS^{4-} system were almost consistent with the bulk organic spectrum at $-0.21\,V \le \Delta_o^w\phi \le 0.31\,V$ (**Figure 7b**), whereas the anionic H_2TPPS^{4-} species should exist stably in the aqueous phase at $\Delta_o^w\phi^{o'}_{H_2TPPS^{4-}} < \Delta_o^w\phi$. It should be noted that the PM-TIRF intensity at given potentials in **Figure 7b** showed essentially the same potential dependence as **Figure 6a**. The PM-TIRF spectra measured for H_2TPPS^{4-} under potentiostatic control indicate that H_2TPPS^{4-} molecules are preferably dehydrated and solvated at the water|DCE interface and then the porphyrin ring could readily be oriented in plane of the interface. In the PM-TIRF measurements, both the molecular orientation and spectral feature of the interfacial species are investigated without controversial interference from the bulk solution species. As mentioned previously, the PMF spectroscopy has provided valuable information about potential-driven transfer and adsorption dynamics of ionizable fluorescent species in the interfacial region. Although the orientation parameter and spectral characterization are attained by the PMF technique within limited conditions,[21-23] the PM-TIRF technique shows a significant advantage in terms of the characterization of the species adsorbed at the liquid|liquid interface.

CONCLUSIONS

The polarization-modulation total internal reflection fluorescence (PM-TIRF) spectroscopy was developed in this work and applied to study the adsorption behavior of *meso*-substituted water-soluble porphyrins at the polarized water|DCE interface. The potential dependences of the molecular orientation and adsorption state of interfacial species were successfully analyzed by PM-TIRF technique. The average orientation angles of H_2TMPyP^{4+} and H_2TPPS^{4-} at the aqueous side of the interface were estimated at $\theta = 61 \pm 1°$ and $\theta = 65 \pm 1°$, respectively. Furthermore, the PM-TIRF spectra clearly indicated that the free-base porphyrins are adsorbed with a modification of the solvation at the water|DCE interface. These results demonstrated that PM-TIRF spectroscopy is a highly sensitive and selective technique for fluorescent species oriented at a liquid|liquid interface and *in situ* characterization of interfacial species can be achieved without controversial contribution of bulk species. The principle and experimental setup of PM-TIRF spectroscopy is rather simple in comparison with other surface sensitive techniques such as nonlinear spectroscopy and polarized TR-XAFS. The optical setup for PM-TIRF spectroscopy is analogous to the PMF spectroscopy. In principle, PM-TIRF spectroscopy can be applied to any of fluorescencet dye molecules oriented at either polarized or nonpolarized interfaces, while PMF spectroscopy focuses on potential driven processes of dyes at polarized interfces.[27] The information obtained from both techniques are complementary to each other. Consequently, PM-TIRF spectroscopy allows us to access useful spectroscopic information of interfacial species at a molecular level.

Supporting Information: Polarization modulation efficiency of the excitation beam**,** dependences of the fluorescence intensity on the linear polarization of excitation beam and molecular orientation, ac voltammograms for the porphyrins, CVs and PM-TIRF responses of tris(2,2′-bipyridine)ruthenium(II) ($Ru(bpy)_3^{2+}$), and PM-TIRF responses of H_2TMPyP^{4+} in the presence of Span 20.

ACKNOWLEDGMENTS

This work was supported by Grants-in-Aid for Scientific Research (B) (no.25288064) and Scientific Research (C) (no.24550097) from Japan Society for the Promotion of Science (JSPS). We also gratefully acknowledge the Kanazawa University CHOZEN Project for partial support of the research.

REFERENCES

1. Girault, H. H., Electrochemistry at Liquid-Liquid Interfaces. *Electroanal. Chem.* **2010**, *23*, 1-104.

2. Samec, Z., Electrochemistry at the Interface between Two Immiscible Electolyte Solutions (IUPAC Technical Report). *Pure Appl. Chem.* **2004**, *76*, 2147-2180.

3. Volkov, A. G., *Liquid Interfaces in Chemical, Biological, and Pharmaceutical Application*. Marcel Dekker: New York, 2001.

4. Watarai, H.; Teramae, N.; Sawada, S., *Interfacial Nanochemistry*. Kluwer Academic/Plenum Publishers: New York, 2005.

5. Nagatani, H., *In Situ* Spectroscopic Characterization of Porphyrins at Liquid Interfaces. In *Handbook of Porphyrin Science*, Kadish, K. M.; Smith, K. M.; Guilard, R., Eds. World Scientific Publishing Co.: Singapore, 2014; Vol. Volume 34: Harnessing Solar Energy pp 51-96.

6. Perera, J. M.; Stevens, G. W., Spectroscopic Studies of Molecular Interaction at the Liquid-Liquid Interface. *Anal. Bioanal. Chem.* **2009**, *395*, 1019-1032.

7. Okumura, R.; Hinoue, T.; Watarai, H., Ion-Association Adsorption of Water-Soluble Porphyrin at a Liquid-Liquid Interface and an External Electric Field Effect on the Adsorption. *Anal. Sci.* **1996**, *12*, 393-397.

8. Ishizaka, S.; Kitamura, N., Time-Resolved Total Internal Reflection Fluorometry Study on Chemical and Structural Characteristics at Water/Oil Interfaces. *Bull. Chem. Soc. Jpn.* **2001**, *74*, 1983-1998.

9. Pant, D.; Girault, H. H., Time-Resolved Total Internal Reflection Fluorescence Spectroscopy: Part I. Photophysics of Coumarin 343 at Liquid/Liquid Interface. *Phys. Chem. Chem. Phys.* **2005**, *7*, 3457-3463.

10. Eisenthal, K. B., Liquid Interfaces Probed by Second-Harmonic and Sum-Frequency Spectroscopy. *Chem. Rev.* **1996**, *96*, 1343-1360.

11. Corn, R. M.; Higgins, D. A., Optical Second Harmonic Generation as a Probe of Surface Chemistry. *Chem. Rev.* **1994**, *94*, 107-125.

12. Benjamin, I., Static and Dynamic Electronic Spectroscopy at Liquid Interfaces. *Chem. Rev.* **2006**, *106*, 1212-1233.

13. Sutherland, R. L., *Handbook of Nonlinear Optics*, 2nd ed.; Marcel Dekker: New York, 2003.

14. Boyd, R. W., *Nonlinear Optics*, 3rd ed.; Academic Press: London, 2008.

15. Roy, S.; Covert, P. A.; Fitzgerald, W. R.; Hore, D. K., Biomolecular Structure at Solid-Liquid Interfaces as Revealed by Nonlinear Optical Spectroscopy. *Chem. Rev.* **2014**, *114*, 8388-8415.

16. Zaera, F., Surface Chemistry at the Liquid/Solid Interface. *Surf. Sci.* **2011**, *605*, 1141-1145.

17. Nagatani, H.; Sagara, T., Potential-Modulation Spectroscopy at Solid/Liquid and Liquid/Liquid Interfaces. *Anal. Sci.* **2007**, *23*, 1041-1048.

18. Sagara, T., UV-visible Reflection Spectroscopy of Thin Organic Films at Electrode Surfaces. In *Diffraction and Spectroscopic Methods in Electrochemistry*, Alkire, R. C.; Kolb, D. M.; Lipkowski, J.; Ross, P. N., Eds. Wiley-VCH: Weinheim, 2006; pp 47-95.

19. Fermín, D. J.; Ding, Z.; Brevet, P. F.; Girault, H. H., Potential-Modulated Reflectance Spectroscopy of the Methyl Orange Transfer across the Water|1,2- Dichloroethane Interface. *J. Electroanal. Chem.* **1998**, *447*, 125-133.

20. Fermín, D. J., Linear and Non-Linear Spectroscopy at the Electrified Liquid/Liquid Interface. In *Diffraction and Spectroscopic Methods in Electrochemistry*, Alkire, R. C.; Kolb, D. M.; Lipkowski, J.; Ross, P. N., Eds. Wiley-VCH: Weinheim, 2006; pp 127-161.

21. Nagatani, H.; Iglesias, R. A.; Fermín, D. J.; Brevet, P. F.; Girault, H. H., Adsorption Behavior of Charged Zinc Porphyrins at the Water/1,2-Dichloroethane Interface Studied by Potential Modulated Fluorescence Spectroscopy. *J. Phys. Chem. B* **2000**, *104*, 6869-6876.

22. Nagatani, H.; Ozeki, T.; Osakai, T., Direct Spectroelectrochemical Observation of Interfacial Species at the Polarized Water/1,2-Dichloroethane Interface by Ac Potential Modulation Technique. *J. Electroanal. Chem.* **2006**, *588*, 99-105.

23. Osakai, T.; Yamada, H.; Nagatani, H.; Sagara, T., Potential-Dependent Adsorption of Amphoteric Rhodamine Dyes at the Oil/Water Interface as Studied by Potential-Modulated Fluorescence Spectroscopy. *J. Phys. Chem. C* **2007**, *111*, 9480-9487.

24. Nagatani, H.; Sakamoto, T.; Torikai, T.; Sagara, T., Encapsulation of Anilinonaphthalenesulfonates in Carboxylate-Terminated PAMAM Dendrimer at the Polarized Water|1,2-Dichloroethane Interface. *Langmuir* **2010**, *26*, 17686-17694.

25. Yoshimura, T.; Nagatani, H.; Osakai, T., Combined Use of Two Membrane-Potential-Sensitive Dyes for Determination of the Galvani Potential Difference across a Biomimetic Oil/Water Interface. *Anal. Bioanal. Chem.* **2014**, *406*, 3407-3414.

26. Sakae, H.; Nagatani, H.; Imura, H., Ion Transfer and Adsorption Behavior of Ionizable Drugs Affected by PAMAM Dendrimers at the Water|1,2- Dichloroethane Interface. *Electrochim. Acta.* **2016**, *191*, 631-639.

27. Nagatani, H.; Fermín, D. J.; Girault, H. H., A Kinetic Model for Adsorption and Transfer of Ionic Species at Polarized Liquid|Liquid Interfaces as Studied by Potential Modulated Fluorescence Spectroscopy. *J. Phys. Chem. B* **2001**, *105*, 9463-9473.

28. Blaudez, D.; Castano, S.; Desbat, B., PM-IRRAS at Liquid Interfaces. In *Biointerface Characterization by Advanced IR Spectroscopy*, Elsevier: 2011; pp 27-55.

29. Blaudez, D.; Buffeteau, T.; Cornut, J. C.; Desbat, B.; Escafre, N.; Pezolet, M.; Turlet, J. M., Polarization Modulation FTIR Spectroscopy at the Air-Water Interface. *Thin Solid Films* **1994**, *242*, 146-150.

30. Cornut, I.; Desbat, B.; Turlet, J. M.; Dufourcq, J., In Situ Study by Polarization Modulated Fourier Transform Infrared Spectroscopy of the Structure and Orientation of Lipids and Amphipathic Peptides at the Air-Water Interface. *Biophys. J.* **1996**, *70*, 305-312.

31. Buffeteau, T.; Blaudez, D.; Pere, E.; Desbat, B., Optical Constant Determination in the Infrared of Uniaxially Oriented Monolayers from Transmittance and Reflectance Measurements. *J. Phys. Chem. B* **1999**, *103*, 5020-5027.

32. Mendelsohn, R.; Flach, C. R., Infrared Reflection-Absorption Spectroscopy of Lipids, Peptides, and Proteins in Aqueous Monolayers. In *Curr. Top. Membr.*, 2002; Vol. 52, pp 57-88.

33. Tanida, H., Total-Reflection X-Ray Absorption Fine Structure on Liquid Surface. *Spectrochim. Acta B* **2004**, *59*, 1071-1076.

34. Watanabe, I.; Tanida, H.; Kawauchi, S., Coordination Structure of Zinc(II) Ions on a Langmuir Monolayer, Observed by Total-Reflection X-Ray Absorption Fine Structure. *J. Am. Chem. Soc.* **1997**, *119*, 12018-12019.

35. Watanabe, I.; Tanida, H.; Kawauchi, S.; Harada, M.; Nomura, M., X-Ray Absorption Spectroscopy of Liquid Surface. *Rev. Sci. Instrum.* **1997**, *68*, 3307-3311.

36. Nagatani, H.; Tanida, H.; Ozeki, T.; Watanabe, I., Zinc(II) Porphyrins at the Air-Water Interface as Studied by Polarized Total-Reflection X-Ray Absorption Fine Structure. *Langmuir* **2006**, *22*, 209-212.

37. Nagatani, H.; Tanida, H.; Watanabe, I.; Sagara, T., Extended X-Ray Absorption Fine Structure of Copper(II) Complexes at the Air-Water Interface by a Polarized Total-Reflection X-Ray Absorption Technique. *Anal. Sci.* **2009**, *25*, 475-480.

38. Nagatani, H.; Tanida, H.; Harada, M.; Asada, M.; Sagara, T., Polarized Total-Reflection X-Ray Absorption Fine Structure of Zinc(II) Porphyrin at the Heptane-Water Interface. *J. Phys. Chem. C* **2010**, *114*, 18583-18587.

39. Wandlowski, T.; Marecek, V.; Samec, Z., Galvani Potential Scales for Water-Nitrobenzene and Water-1,2-Dichloroethane Interfaces. *Electrochim. Acta.* **1990**, *35*, 1173-1175.

40. Ohta, N.; Matsunami, S.; Okazaki, S.; Yamazaki, I., Polarized Absorption Spectra and Molecular Orientation of Some Cyanine Dyes in Langmuir-Blodgett Monolayer Films. *Langmuir* **1994**, *10*, 3909-3912.

41. Akutsu, H.; Kyogoku, Y.; Nakahara, H.; Fukuda, K., Conformational Analysis of Phosphatidylethanolamine in Multilayers by Infrared Dichroism. *Chem. Phys. Lipids* **1975**, *15*, 222-242.

42. Nagatani, H.; Piron, A.; Brevet, P. F.; Fermín, D. J.; Girault, H. H., Surface Second Harmonic Generation of Cationic Water-Soluble Porphyrins at the Polarized Water. *Langmuir* **2002**, *18*, 6647-6652.

43. Improta, R.; Ferrante, C.; Bozio, R.; Barone, V., The Polarizability in Solution of Tetra-Phenyl-Porphyrin Derivatives in Their Excited Electronic States: A PCM/TD-DFT Study. *Phys. Chem. Chem. Phys.* **2009**, *11*, 4664-4673.

44. Kakiuchi, T., Potential-Dependent Adsorption and Partitioning of Ionic Components at a Liquid|Liquid Interface. *J. Electroanal. Chem.* **2001**, *496*, 137-142.

45. Piron, A.; Brevet, P. F.; Girault, H. H., Surface Second Harmonic Generation Monitoring of the Anion Methyl Orange During Ion Transfer Reactions across a Polarized Water. *J. Electroanal. Chem.* **2000**, *483*, 29-36.

46. Kano, K.; Nakajima, T.; Takei, M.; Hashimoto, S., Self Aggregation of Cationic Porphyrin in Water. *Bull. Chem. Soc. Jpn.* **1987**, *60*, 1281-1287.

47. Wang, H.; Borguet, E.; Eisenthal, K. B., Polarity of Liquid Interfaces by Second Harmonic Generation Spectroscopy. *J. Phys. Chem. A* **1997**, *101*, 713-718.

48. Wang, H.; Borguet, E.; Eisenthal, K. B., Generalized Interface Polarity Scale Based on Second Harmonic Spectroscopy. *J. Phys. Chem. B* **1998**, *102*, 4927-4932.

49. Steel, W. H.; Walker, R. A., Measuring Dipolar Width across Liquid-Liquid Interfaces with 'Molecular Rulers'. *Nature* **2003**, *424*, 296-299.

50. Steel, W. H.; Beildeck, C. L.; Walker, R. A., Solvent Polarity across Strongly Associating Interfaces. *J. Phys. Chem. B* **2004**, *108*, 16107-16116.

51. Siler, A. R.; Brindza, M. R.; Walker, R. A., Hydrogen-Bonding Molecular Ruler Surfactants as Probes of Specific Solvation at Liquid/Liquid Interfaces. *Anal. Bioanal. Chem.* **2009**, *395*, 1063-1073.

52. Benjamin, I., Reaction Dynamics at Liquid Interfaces. *Annu. Rev. Phys. Chem.* **2015**, *66*, 165-188.

53. Nagatani, H.; Samec, Z.; Brevet, P. F.; Fermín, D. J.; Girault, H. H., Adsorption and Aggregation of *meso*-Tetrakis(4-Carboxyphenyl)Porphyrinato Zinc(II) at the Polarized Water|1,2-Dichloroethane Interface. *J. Phys. Chem. B* **2003**, *107*, 786-790.

TOC graphic

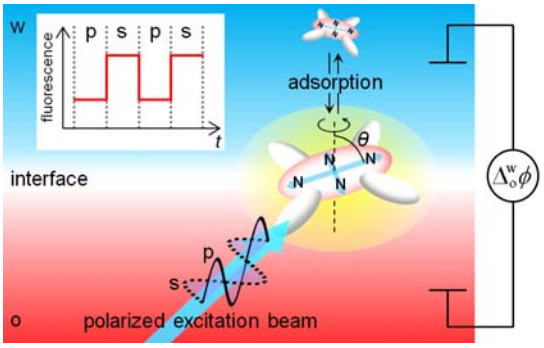
w
p
s
p
s
fluorescence
t
adsorption
θ
N
N
N
N
interface
p
s
o
polarized excitation beam
$\Delta_o^w\phi$